Pharm Res (2011) 28:1306–1316
DOI 10.1007/s11095-010-0358-5

RESEARCH PAPER

Porous EH and EH-PEG Scaffolds as Gene Delivery Vehicles to Skeletal Muscle

Erin E. Falco • Martha O. Wang • Joshua A. Thompson • Joshua M. Chetta • Diana M. Yoon • Erik Z. Li • Mangesh M. Kulkami • Sameer Shah • Abhay Pandit • J. Scott Roth • John P. Fisher

Received: 1 October 2010 / Accepted: 17 December 2010 / Published online: 19 January 2011

ABSTRACT

Purpose Synthetic biomaterials are widely used in an attempt to control the cellular behavior of regenerative tissues. This can be done by altering the chemical and physical properties of the polymeric scaffold to guide tissue repair. This paper addresses the use of a polymeric scaffold (EH network) made from the cyclic acetal monomer, 5-ethyl-5-(hydroxymethyl)-β,β-dimethyl-1,3-dioxane-2-ethanol diacrylate (EHD), as a release device for a therapeutic plasmid encoding for an insulin-like growth factor-1 green fluorescent protein fusion protein (IGF-1 GFP).

Methods Scaffolds were designed to have different porous architectures, and the impact of these architectures on plasmid release was determined. We hypothesized that IGF-1 could be delivered more effectively using a porous scaffold to allow for the release of IGF-1.

Results We showed that by altering the number of pores exposed to the surface of the network, faster plasmid loading and release were achieved. In addition, the IGF-1 GFP plasmids were found to be effective in producing IGF-1 and GFP within human skeletal muscle myoblast cell cultures.

Conclusions This work aims to show the utility of EH biomaterials for plasmid delivery for potentially localized skeletal muscle regeneration.

KEY WORDS cyclic acetal · gene therapy · IGF-1 · synthetic meshes

INTRODUCTION

At an ever increasing pace, synthetic biomaterials are being developed with specific functionalities for tissue engineering applications (1–3). Synthetic polymers are often chosen over natural polymers for their versatile and tunable chemical and physical properties. These biomaterial scaffolds can be created to guide or direct cell attachment and migration as well as deliver therapeutic proteins, viruses, and plasmids to recreate a specific tissue (4,5). Attempts to control these cell functions and release patterns have led to the development of scaffolds with various surface and bulk architectures (6–8). This paper focuses on creating cyclic acetal porous single-component and bi-component scaffolds from 5-ethyl-5-(hydroxymethyl)-β,β-dimethyl-1,3-dioxane-2-ethanol diacrylate (EHD) and polyethylene glycol (PEG). These scaffolds are to be used as a delivery device for a therapeutic plasmid that produces an insulin-like growth factor-1 and green florescent proteins (IGF-1 GFP).

E. E. Falco
Department of Chemical and Biomolecular Engineering
University of Maryland
College Park, Maryland, USA

M. O. Wang • J. A. Thompson • J. M. Chetta • E. Z. Li • S. Shah • J. P. Fisher (✉)
Fischell Department of Bioengineering, University of Maryland
3238 Jeong H. Kim Building
College Park, Maryland 20742, USA
e-mail: jpfisher@umd.edu
URL: http://www.terpconnect.umd.edu/~jpfisher

D. M. Yoon
Department of Bioengineering, Rice University
Houston, Texas, USA

M. M. Kulkami • A. Pandit
National Centre for Biomedical Engineering Science
National University of Ireland
Galway, Ireland

J. S. Roth
Department of Surgery, University of Kentucky College of Medicine
Lexington, Kentucky, USA

Cyclic acetal biomaterials are polymeric networks that are formed from the chemical crosslinking of the six member ring structured cyclic acetal unit. This unit is formed from and later degrades (via hydrolysis) into diol and carbonyl end groups (9,10). Therefore, this monomer has the potential to eliminate the acidic byproducts commonly associated with ester-based biomaterials (11). In these studies, a cyclic acetal containing diacrylate end groups (EHD) was used to form biomaterial (EH) scaffolds. One drawback to this material is that while the backbone of the EH scaffolds is formed from these hydrolytically degradable units, the use of the diacrylate end groups creates an additional carboxylic acid byproduct which can affect the local *in vivo* environment. These effects are minimal, however, making this polymer a strong candidate for biomedical applications (9,10,12–14).

This paper evaluates the delivery of IGF-1 GFP from EH scaffold to skeletal muscle cells. Previous work has shown that EH scaffolds can be used as a regenerative scaffold for skeletal muscle (13). Other studies have shown that exogenously delivered IGF-1 to myoblasts, seeded on EH scaffolds, showed an increase in growth and proliferation (13). Skeletal muscle has been extensively studied for gene therapy applications and has been shown to be compatible with EH scaffolds (13,15). Many trials evaluate skeletal muscle as a mechanism to continuously distribute secreted therapeutic proteins systemically for the treatment of muscular genetic diseases and ischemia as well as for DNA vaccines (15,16). These studies have shown some success; however, the biggest challenges stem from low transfection efficiency and only localized protein production. While these hurdles hinder gene therapy for traditional myopathies, they can be utilized to treat pathologies that do not require systemic protein infusion.

Insulin-like growth-factor 1 (IGF-1) is a main protein in skeletal muscle regeneration (17). It has been shown that IGF-1 functions as both an autocrine and paracrine signal which affects skeletal muscle growth and development (18–21). Specifically, IGF-1 binds to activated satellite cells which are able to differentiate into new muscle fibers or augment existing fibers (22). IGF-1 also increases both cell proliferation and differentiation (20,23,24). Increasing IGF-1 levels in skeletal muscle lead to an increase in both DNA and protein content within the target muscle (23). Additionally, IGF-1 is known to modulate the expression of cytokines, e.g. tumor necrosis factor alpha, and interleukin-1 beta, decreasing the time needed for muscle regeneration (21). Therefore, it is believed that IGF-1 may be critical for activating and guiding satellite cell behavior in skeletal muscle regeneration (20).

Currently, both viral and nonviral vectors have been studied for the delivery of IGF-1. Although viral transfection is effective for delivering cells, concerns regarding an immunological response have led researchers to evaluate nonviral methods for gene transfection (25). However, some nonviral methods suffer from a lack of long-term delivery of the desired gene (26). The following studies explore the initial stages of creating a therapeutic plasmid and a polymeric release system. Specifically, the *in vitro* transfection efficiency and release patterns of an IGF-1 GFP plasmid from porous single-component and bi-component scaffolds formed from 5-ethyl-5-(hydroxymethyl)-β,β-dimethyl-1,3-dioxane-2-ethanol diacrylate (EHD) and polyethylene glycol (PEG) were investigated. EH scaffolds' ability to function as regenerative scaffold for myoblasts, partnered with an increased production of IGF-1 through gene therapy could allow for EH scaffolds to act as both a long- and short-term therapy. We believe the combination of porous EH scaffold to deliver nonvirally the IGF-1 gene will function as the next step to resolve some of these issues.

MATERIALS AND METHODS

Benzoyl peroxide (BP), N,N-dimethyl-p-toluidine (DMT), 5-ethyl-5-(hydroxymethyl)-β,β-dimethyl-1,3-dioxane-2-ethanol diacrylate (EHD), isobutyraldehyde, formaldehyde (37% aqueous solution), trimethylolpropane, triethylamine, hydroquinone, acryloyl chloride, ammonium persulfate (APS), N,N,N′,N′-tetramethylethylenediamine (TEMED), PEG diacrylate (PEGDA), agar, agarose powder and LB media were obtained from Sigma-Aldrich (Milwaukee, WI, USA). Reagent grade acetone, potassium carbonate, sodium sulfate, ethyl ether, silica gel (60–200 mesh) and sodium chloride (salt) were purchased from Fisher Scientific (Pittsburgh, PA, USA). One kb DNA ladder and *EcoNI* restriction enzyme were ordered from New England Biolabs, Ipswich, MA, USA. Lipofectin Transfection Reagent, Opti-MEM I Reduced Serum Media (Opti-MEM), Vivid Colors™ pcDNA™ 6.2/C-EmGFP-GW/TOPO® Mammalian Expression Vector, One Shot® TOP10 chemically competent E. coli, Lipofectamine 2000 Transfection Reagent and SYBR® safe DNA gel stain were received from Invitrogen (Carlsbad, CA, USA). FuGENE Transfection Reagent was purchased from Roche Applied Science (Indianapolis, IN, USA) and Promega (Madison, WI, USA). Human skeletal muscle myoblasts (hSkMM), skeletal muscle cell growth media and BulletKit, trypsin/EDTA and trypsin neutralization solution were obtained from Lonza (Walkersville, MD, USA).

5-Ethyl-5-(Hydroxymethyl)-β,β-Dimethyl-1,3-Dioxane-2-Ethanol Diacrylate Synthesis

EHD was synthesized based on the protocols described by Kaihara *et al.* (12). Potassium carbonate (18.9 g, 0.25 equiv) was added to isobutyraldehyde (50 mL, 1 equiv) and

formaldehyde (37% aqueous solution, 40.8 mL, 1 equiv), and the resulting solution was stirred at 0°C overnight. The product 3-hydroxy-2,2-dimethylpropinaldehyde (HDP) was extracted three times with chloroform and then washed with water and brine. The chloroform layers were combined and dried with sodium sulfate, and the solvent was evaporated under reduced pressure to obtain solid HDP. HDP (32.9 g, 1 equiv) and trimethylolpropane (86.6 g, 2 equiv) were dissolved in 1 M hydrochloric acid (200 mL) and stirred for 2 h at 80°C. The solution was then neutralized with sodium hydroxide, and the product 5-ethyl-5-(hydroxymethyl)-β,β-dimethyl-1,3-dioxane-2-ethanol (HEHD) was extracted three times with chloroform and washed with water and brine. The chloroform layers were combined and again dried with sodium sulfate and evaporated under reduced pressure to obtain solid HEHD. The HEHD was purified using an ethyl ether wash to remove undesired byproducts and was dried under reduced pressure. HEHD (31.3 g, 1 equiv) was dissolved in chloroform, and triethylamine (65.4 mL, 3 equiv) and hydroquinone (0.034 g, 0.002equiv) were added. Acryloyl chloride (38.1 mL, 3 equiv) was added drop-wise as the reaction was stirred at 0°C for 2 h. The insoluble salts were removed through filtration, and the product, EHD, was extracted three times with chloroform and washed with water and brine. The chloroform layers were combined and dried with sodium sulfate and evaporated under reduced pressure. The EHD was further purified by silica gel column chromatography using a chloroform/ethanol (10:1, v/v) as the eluent. The fractions that contained EHD were determined by thin layer chromatography and NMR.

Solution Formed Porous EH Scaffold Formation

Solution-formed porous EH networks (EH scaffolds) were made using a leachable porogen strategy. Rectangular cavities with dimensions of 7 cm×4.3 cm were cut from 1.4 mm thick plastic sheets to form frames. A glass plate was placed under the frames to form a well, which was filled with 7.8 g of salt. Salt was wetted with 2.4 mL 85% acetone and spread with another glass plate to fill the frame. Salt-filled frames were dried on an 85°C hot plate for 1 h to produce an interconnected salt network that was attached to the plastic frame. The salt-filled frame was allowed to cool 10 min before removal from the glass plate.

The mass of the salt network was measured to determine the amount of polymer solution required to achieve 75 and 80 wt% salt porosities. Active EHD solution was prepared by mixing each gram of EHD with 375 µL of 0.826 M BP in acetone and 8 µL DMT. The salt-filled frame was suspended over a weighing dish such that the salt network was solely supported by the frame and active EHD solution was delivered drop-wise onto the salt cake.

The frame was then placed in a 60°C oven for 20 min to promote polymer gelling. Once gelled, the EH scaffolds were transferred to DI water to leach out salt. After 20 min, the networks were removed from the frame to prevent cracking, and the salt was leached out for 48 h with a water change at 24 h.

EH-PEG Bi-Component Scaffold Production

EH scaffolds were made as described. Networks were removed from the water after 48 hours and dried overnight at ambient temperature and pressure. Twenty-mM solutions of the water-soluble radical initiators ammonium persulfate (APS) and N,N,N′,N′-tetramethylethylenediamine (TEMED) were made as well as a 30% solution of PEG diacrylate (PEGDA) in 5% acetone. Two stacks of three coverslips were placed on a glass plate to control the thickness of the PEGDA layer on the EH scaffold. After combining the PEGDA, APS, and TEMED, the solution was vortexed and poured quickly in between the coverslips. The dried EH scaffold was placed on top of the coverslips, and the PEGDA was allowed to crosslink with the network. After the PEGDA was gelled, the network was removed from the plate, and the excess PEG was removed. The EH-PEG bi-component scaffolds (EH-PEG scaffold) could then be cut into any desired shape.

Scanning Electron Microscopy (SEM)

EH and EH-PEG scaffolds were fabricated as mentioned previously. The top surface and cross-section of each scaffold was coated with gold prior to imaging. Images were obtained using a Hitachi Field Emission Scanning Electron Microscope fitted with an X-Ray Analysis System.

IGF-1 GFP Fusion Plasmid Construction

To produce the IGF-1 GFP fusion plasmid (Fig. 1), RNA was isolated from human skeletal muscle myoblasts (hSkMMs). cDNA was created using reverse transcription, and the IGF-1 gene was amplified by performing a polymerase chain reaction (PCR). The PCR product was then purified through agarose gel electrophoresis, and the desired cDNA was removed from the gel. This product was mixed with the Vivid Colors™ pcDNA™ 6.2/C-EmGFP-GW/TOPO® Mammalian Expression Vector and then used to transform One Shot® TOP10 chemically competent *E. coli*. The cells were spread onto agar plates containing 100 µg/mL of ampicillin and were left in the incubator at 37°C for 12–14 h, at which time they were moved to 4°C for storage. Colonies were chosen from the plates and grown in LB media containing 100 µg/mL of ampicillin for 12–16 hours. Using a Promega Endotoxin Free Midi Prep Kit, the plasmid was harvested from the

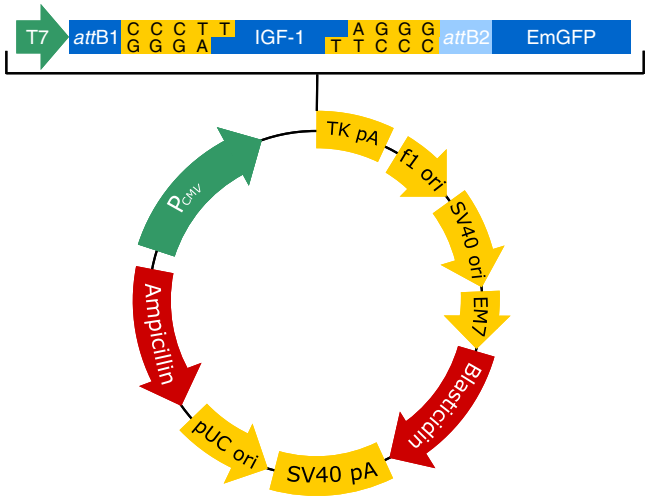

Fig. 1 Plasmid vector map for the insulin-like growth factor I green fluorescent protein plasmid (adapted from Invitrogen Vivid Color™ pcDNA™ 6.2/N-EmGFP-GW/TOPO® Mammalian Expression Vector Map, Cat. No. K360-20).

cells, and concentration was determined using the NanoDrop spectrophotometer. To ensure proper insertion of the PCR product into the TOPO vector, the inserted product was amplified using PCR and purified using gel electrophoresis. The sample was then sent to DNA sequencing to confirm presence of IGF-1 gene.

Fusion Gene Complex Formation

Fusion gene complexes (FG complex) were formed using the FuGENE Transfection Reagent. DNA was diluted in Opti-MEM to a concentration of 2 ng/100 µL. FuGENE was then added to the solution at a ratio of 6:2 (FuGENE (µL):DNA(µg)) and gently mixed. The solution was incubated at room temperature for 15 min before use.

Fusion Gene Lipoplex Formation

Fusion gene lipoplexes (lipoplexes) were formed using the Lipofectamine 2000 Transfection Reagent. First, the required amount of DNA was diluted in 50 µL of Opti-MEM. Then, Lipofectamine 2000 was diluted in 50 µL of Opti-MEM in a ratio of 6:2 (Lipofectamine 2000:DNA). After a 5 min incubation at room temperature, the DNA was added to the Lipofectamine 2000, and the lipoplexes were incubated at room temperature for an additional 20 min before use.

IGF-1 Plasmid Integrity After Release from EH Scaffolds

Plasmid DNA released from EH scaffolds was evaluated for intactness and inclusion of the IGF-1 gene. EH 75 wt% scaffolds were formed, pre-wetted and sterilized prior to being placed into a 12-well plate. The scaffolds were submerged in 100% ethanol for 20 min and placed under a vacuum for sterilization. While in a biosafety hood, all the residual ethanol was removed from the scaffolds with five 20-min PBS washes. The scaffolds were then placed in a 12-well plate. Scaffolds were then loaded with 12 µg plasmid DNA or 12 µg plasmid DNA and FG complex in 180 µL of Opti-MEM/plasmid solution. After the plasmid was allowed to absorb onto the scaffolds for 2 h; 340 µL of water was added to the scaffolds to be digested and 250 µL Opti-MEM and 90 µL Type I loading dye were added to all remaining scaffolds. After an additional four hours the *EcoNI* restriction enzyme was added to the scaffolds for digestion for an hour. The solution from all scaffolds was collected after a total of 7 h post plasmid loading and assayed on the 1% agarose gel. As reference, FG complex as well as stock plasmid DNA were placed into Opti-MEM media for 7 h with the addition of the Type I loading dye after the first 2 h.

Stock plasmid in nuclease-free water, stock plasmid digested with the *EcoNI* restriction enzyme, and plasmid released from the scaffold and then *EcoNI* digested were assayed. *EcoNI* was chosen, as the enzyme is specific for a single cut site on the IGF-1 gene insert and does not cut the plasmid vector. Samples not loaded and released from the scaffold contained 500 ng of plasmid DNA. Much less DNA was needed from the unreleased samples in comparison to the loaded scaffolds to obtain the same final concentration of released DNA for loading onto the gel. These samples were compared using 1% agarose gel electrophoresis. A 1 kb DNA ladder was used to evaluate migrated DNA size.

Adsorption Mapping of FG Complex Loading

EH scaffolds and EH-PEG scaffolds, in a 12-well plate, had 188 µL or 140 µL of FG complex, respectively, added drop-wise to the scaffolds. The total available pore volume was calculated using difference in the total volume of the scaffold expected scaffold weight from the actual scaffold weight with the assumption that EH has a density of approximately 1 g/cm^3.

The FG complex solution was allowed to fill the pores. After 6 h, the scaffolds were moved into separate wells, divided into three concentric rings, with one section per well. Then, 500 µL of RNAase-free water was added to the top of each scaffold section. PicoGreen®, a fluorescent nucleic acid stain for quantitating double-stranded DNA, was then used to determine how much of the initially loaded plasmid DNA and complex was absorbed into each ring. A serial dilution of PicoGreen® was created along with a negative control of 0 pg/µl of DNA. The serial dilution, negative control and DNA from each of the segments were then plated on a black fluorescent plate and incubated at room temperature for 2–5 min. The fluores-

cence of the plate was then read, and the DNA concentrations were calculated based on the standard curve. The total amount of DNA per segment was determined as a function of the total volume of the segment.

Transfection Efficiency and Dose Dependence

The plasmid transfection efficiency and dose dependence were evaluated using primary hSkMMs cultured to passage four (p4). The hSkMMs were seeded in a 24-well plate at a density of 60,000 cells per well (approximately 80%–90% confluence). Opti-MEM with FG complexes or lipoplexes was added to the hSkMMs at concentrations of 0.5, 1.0 and 5.0 μg of plasmid DNA per well. Opti-MEM was used as a control. After transfection, the media was changed per the manufacturer's instructions. The hSkMM production of IGF-1, 46 h post-transfection, was assayed using an IGF-1 Quantikine ELISA (R&D Systems, Minneapolis, MN).

Architecture-Guided FG Complex Release

EH scaffolds and EH-PEG bi-component scaffolds with two different porosities were formed as mentioned above. Before seeding the networks they were pre-wetted and sterilized as described above. The networks, were then placed in a 12-well plate, and the FG complex solution was added to the top surface of the scaffolds. The solution was allowed to fill the pores, and any displaced PBS was collected for loading efficiency calculations. Then, 1.4 mL of PBS was added to completely submerge each network. At each time point, 400 μL of PBS was removed and replaced with fresh PBS to maintain a constant volume. PicoGreen® was then used to determine the concentration of the released DNA.

FACS Evaluation of Transfection Efficiency

Fluorescence-activated cell sorting (FACS) was used to further characterize hSkMM transfection efficiency when using FG complex. hSkMMs were transfected using a 6:2 ratio of μg plasmid DNA to μl FuGENE complex per manufacturer guidelines and optimized transfection studies for hSkMM (27). T-25 flasks of p4 hSkMMs were cultured with plasmid DNA, FuGENE transfection reagent or plasmid DNA and FuGENE complex. Each flask treated received 12 μg plasmid DNA and/or 36 μL FuGENE transfection reagent along with 600 μl of Opti-MEM, combined to make the FG complex solution per the description above. One T-25 flask of p4 hSkMMs was untreated to act as a negative control. The transfection was performed using the same process as delineated above. Forty-six hours post-transfection the cells were evaluated for GFP expression. Cells were suspended using trypsin, centrifuged and resuspended in PBS. Non-transfected, control, hSkMM cell were used to provide gating for appropriate cell size. GFP expression of cells within this gated region was evaluated using BD FACSCanto II Flow Cytometer (Becton Dickinson, Hunt Valley, MD, USA), and the data were analyzed using the BD FACSDiva software.

Statistical Analysis

The data from all experiments were analyzed by one-way analysis of variance (ANOVA), and Tukey's multiple-comparison test was performed to verify the statistical difference between the experimental groups with 95% confidence ($p<0.05$).

RESULTS

The objective of this work was to investigate the utility of porous EH and EH-PEG scaffolds as a plasmid delivery device. To this end, plasmid release was measured as a function of scaffold architecture. Initially, the architecture of the EH scaffold was characterized. To test scaffold utility as a functional release device, plasmids that produced IGF-1 GFP fusion proteins were constructed, and plasmid performance was evaluated. Plasmid loading distribution and IGF-1 intactness after release were evaluated to ensure scaffold could be used as an efficient delivery vehicle. Finally, a release study was performed to test the effect of scaffold architecture on the release rate of a FG complex.

Porous EH and EH-PEG scaffolds were fabricated using a frame method. These scaffolds were imaged to show both the macroscopic structure (Fig. 2a, b, f and g) and the microscopic structure (Fig. 2c, d and e). Figure 2f shows the bi-component scaffold with PEG as the top layer. Figure 2a shows a highly porous surface, which can easily be observed under a 2.5× magnification with a Zeiss Inverted Microscope (Fig. 2b and g). Figure 2c–e showed that the pores appear to be cuboidal with rounded edges and evenly distributed throughout the scaffold.

A comparison study of the released and unreleased plasmid was performed using agarose gel electrophoresis, demonstrating that the released plasmid and FG complex were intact and contained the IGF-1 gene (Fig. 3). The restriction enzyme *EcoNI* was used to cleave the IGF-1 gene and demonstrate the presence of an intact IGF-1 gene in the stock plasmid (Fig. 3d) and the released plasmid (Fig. 3f). Released plasmid (Fig. 3e) was compared to stock plasmid (Fig. 3b); both demonstrated similar migration patterns. Plasmid was combined with Opti-MEM and Type I loading dye as a reference, indicating that neither the Opti-MEM nor the Type I loading dye caused DNA degradation (Fig. 3c). The released FG complex (Fig. 3g) and stock FG complex (Fig. 3h) also had similar migration

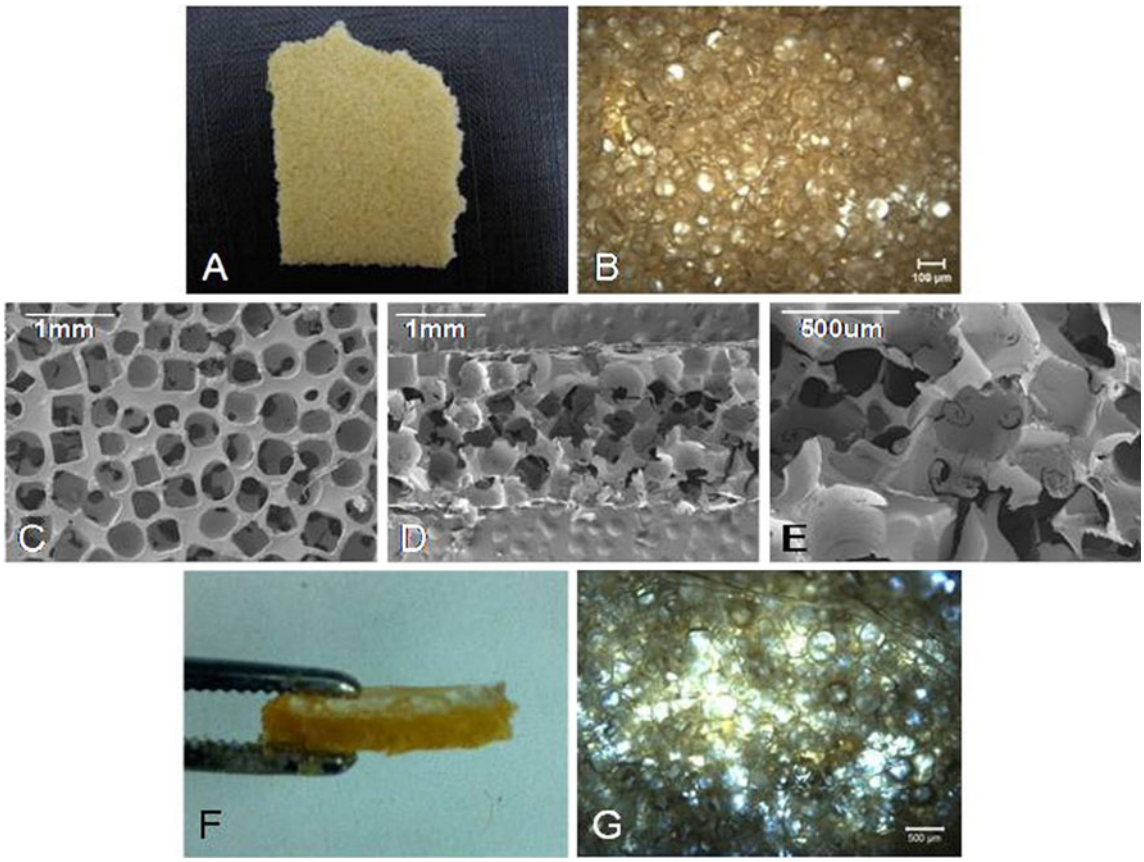

Fig. 2 (**A**) Image of a 75 wt% EH scaffold. (**B**) 2.5× magnification of a 75 wt% EH scaffold. (**C**) SEM image of the surface of a 75 wt% EH scaffold. (**D**) SEM image of the cross-section of a 75 wt% EH scaffold. (**E**) Higher magnification SEM image of a single pore in a 75 wt% EH scaffold. (**F**) Image of 80% EH-PEG scaffold. (**G**) 2.5× magnification of 80% EH-PEG scaffold.

patterns, demonstrating that the complex was not degraded from its interaction with the scaffold.

Prior to evaluating the scaffold entrapment and release efficiency we first characterized the distribution of the plasmid in the scaffold. EH scaffolds were loaded with FG complex and then sectioned into three components to determine physical loading characteristics of each scaffold (Fig. 4). The distribution of the EH scaffold was 32% outer ring, 45% middle ring and 22% in the inner disc, which translated to 0.285%, 1.032% and 1.139% of the total DNA per mm^2 in the outer ring, middle ring and inner disc, respectively. In comparison, the EH-PEG scaffold had a slightly different distribution, with 48%, 31% and 21% in the outer and middle rings and in the inner disc, respectively. This translated to 0.43%, 0.7%, and 1.05% of the total DNA per mm^2 in the outer ring, middle ring and inner disc (Fig. 4b), respectively.

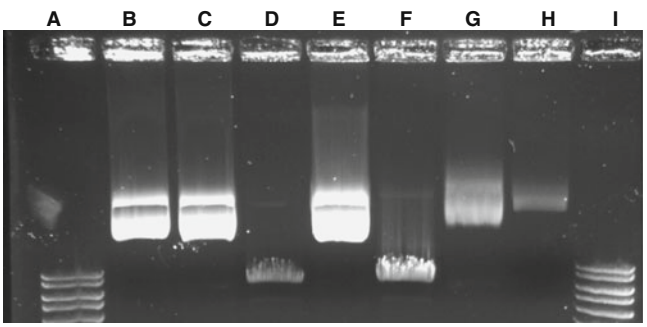

Fig. 3 Gel electrophoresis (1% agarose) of (**A**) 1 kb DNA ladder, (**B**) plasmid stock, (**C**) plasmid in Opti-MEM and Type I loading dye, (**D**) plasmid digested with *EcoNI*, (**E**) plasmid released from scaffold, (**F**) plasmid released from scaffold, digested with *EcoNI*, (**G**) FuGENE complex released from scaffold, (**H**) FuGENE complex, and (**I**) 1 kb DNA ladder. Size of the linearized plasmid was ~6 kb.

After evaluating the scaffold physical characteristics, the next step was the test the efficacy of the hSkMM transfection. Plasmid DNA was created that fused IGF-1 to emGFP to allow for the visual verification of successful IGF-1 gene transfection. This served as a complementary method to the IGF-1 ELISA for evaluating successful transfection. Since high levels of hSkMM transfection efficiency are known to be challenging, two different carriers for fusion gene plasmid delivery were evaluated (28). FuGENE (FG complex) and Lipofectamine 2000 (lipoplexes) were chosen based on their previous successful uses with hSkMM (28). These plasmids were added to

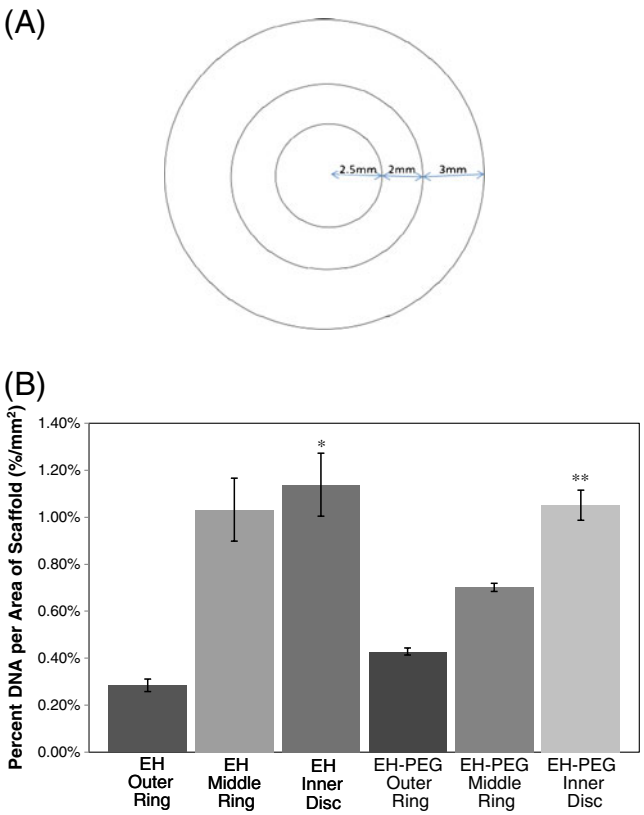

Fig. 4 (**A**) Concentric ring structure of EH and EH-PEG 75 wt% scaffolds. (**B**) Distribution of DNA within scaffold geometry. In both scaffolds the inner segment had a statistically significantly larger percent of DNA compared to the middle and outer segments ($p = 0.05$).

hSkMMs, and 46 h after transfection, IGF-1 concentrations in the supernatant were measured by an ELISA and compared to non-transfected hSkMM IGF-1 levels. Figures 5a–c shows GFP production within cells transfected with FG complexes. Figures 5a and b demonstrate that hSkMMs can produce GFP when seeded at a density of 20,000 and 40,000 cells/well, respectively. Figure 5c indicates successful transfection in fused myoblasts. Figure 5d shows that IGF-1 production appears to only be affected slightly by plasmid dose with a statistically higher amount of protein being produced with the highest concentration of FG complexes, 5.0 μg, compared to the control.

Fluorescent-activated cell sorting was used to qualitatively evaluate the transfection protocol provided by FuGENE HD manufacturer and previous studies (27). T-25 flasks were transfected using 12 μg plasmid DNA and 36 μl FuGENE reagent, whereas three additional T-25 flasks with p4 hSkMM flasks were treated with 12 μg plasmid DNA, 36 μl FuGENE reagent or with Opti-MEM in the same manner as the transfected cells to act as controls. The transfected hSkMM cells showed GFP expression in 11.1% of the population in comparison to 1.2% of the control sample, 0.6% of the DNA only sample, and 3.2% of the FuGENE only sample (Fig. 6).

Once successful transfection, plasmid distribution, and an intact released plasmid were demonstrated from each scaffold, the architecture's impact on plasmid release rates was evaluated. To determine the effects of architecture on the plasmid release rate, both EH scaffolds and EH-PEG scaffolds were fabricated. Complexes were loaded onto the different scaffolds, and DNA concentration in the supernatant was measured over 24 h. Figure 7 shows that the release profile was initiated with a burst release during the first hour, followed by lower release rates up to 24 h. Overall, all groups performed similarly; however, general trends show that the 75 wt% EH scaffolds released more complex over 24 h than its more porous counterpart, the 80 wt% EH scaffold. In addition, the EH-PEG scaffolds retained more complex than the EH scaffolds of the same porosity for the first 2 h. The 75 wt% EH-PEG scaffolds continued to release more than its EH scaffold counterpart; however, the 80 wt% EH scaffold released more than the EH-PEG scaffold after 2 h.

DISCUSSION

In this work, an EH scaffold was developed for the release of IGF-1 GFP fusion plasmids. Previous work has focused on the biocompatibility of the EH scaffolds (13). Skeletal myoblasts were able to attach and proliferate on the scaffolds which were shown to also release active IGF-1 over a 48 h period of time (13).To further this work, it was hypothesized that the IGF-1 gene delivery complex could be delivered more effectively using a porous scaffold to allow for extended release of the IGF-1 complex. Scaffolds were fabricated using a porogen leaching strategy, and SEM photos were taken after leaching to qualitatively determine pore interconnectivity and distribution (Fig. 2). To increase pore distribution of the scaffolds, salt frames were made to maintain porous surfaces. Interconnectivity was also established quantitatively by monitoring the mass lost during leaching. The 80 wt% EH scaffolds lost 86.67%±0.64% of their overall mass after 48 h. In these samples, the mass that was lost was greater than the amount of porogen added. It is speculated that this is due to the removal of unreacted monomers and initiator during leaching. As can be seen in Fig. 2, EH scaffolds were fabricated with increased number of pores exposed at the surface as well as throughout the cross-section.

Next, we modified the scaffold architecture by coating one side of the porous scaffolds with a layer of PEG to change scaffold release kinetics. We hypothesized that adding a PEG layer to one surface of the scaffold would

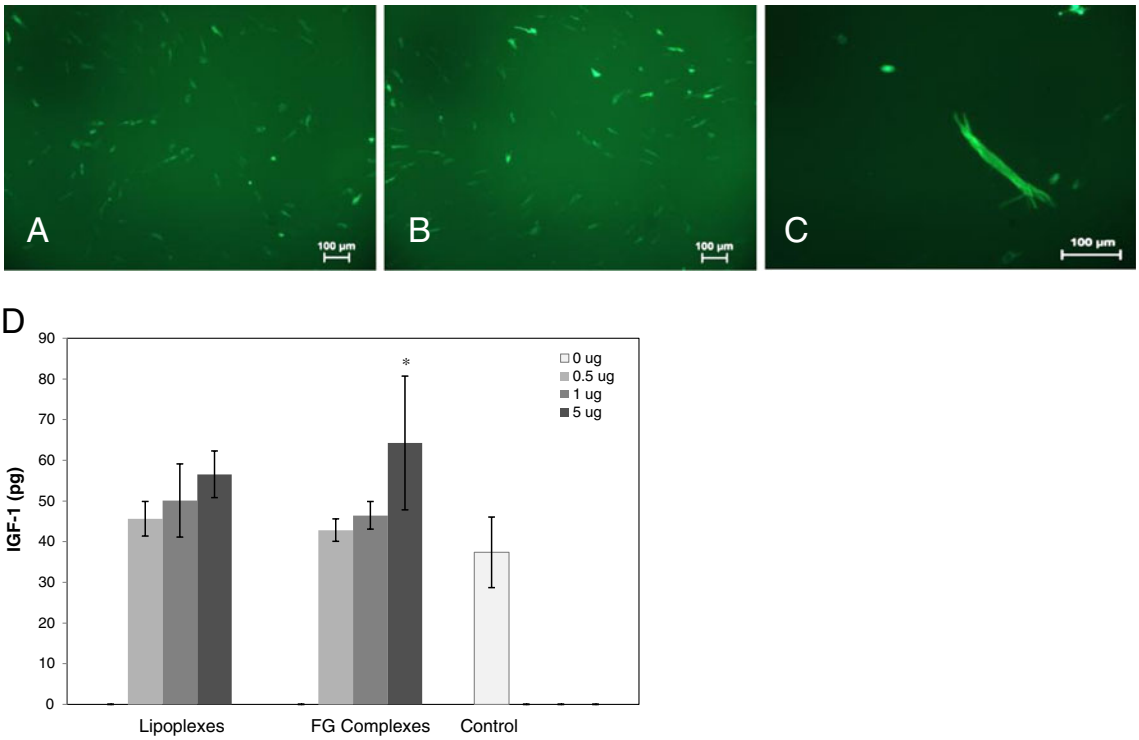

Fig. 5 (**A**) GFP expression within hSkMMs seeded at a density of 20,000 cells/well. (**B**) GFP expression within hSkMMs seeded at a density of 40,000 cells/well. (**C**) GFP expression within fused hSkMMs in culture. (**D**) Amount of IGF-1 produced from transfected hSkMMs. The general trend shows that there is a slight dose response over the DNA range used. In addition, the lipoplexes and the complexes performed similarly at all doses. The 5 μg FuGENE complex group was statistically higher than the control group ($p = 0.05$).

block those pores and enhance the scaffold's loading and release efficiencies. Delivery of the IGF-1 gene to the myoblasts was enhanced through gene therapy techniques. Gene delivery is a promising tool in producing therapeutic proteins within skeletal muscle (11,15). Liposomal carriers were chosen over naked DNA due to the known difficulty of transfecting primary skeletal myoblasts (29).

Adsorption mapping of the FG complexes onto the scaffold was accomplished by segmenting loaded scaffolds into three parts and then assaying DNA concentrations using PicoGreen®. This study elucidated the distribution of plasmid during loading and worked to ensure that the interconnected pore architecture of the EH and EH-PEG scaffolds allows for even distribution of the plasmid for its eventual release into surrounding cells. As the FG complex was added drop-wise to the top of the scaffold, it is intuitive that the largest concentration of DNA would be present at the center of the scaffold. Although both scaffolds had the highest percent of the total DNA per area in the inner disc, the EH-PEG scaffold had a larger percent of DNA in both its outer and middle rings compared to the EH-scaffold. This allows us to believe that the formation of the PEG layer on the EH scaffold allowed for more of the DNA to migrate through the porous network. Though the distribution was not completely even, the distribution of the DNA was within 1% difference between each section of the scaffold, which we speculate would not significantly impact release rate kinetics.

Intactness of the IGF-1 gene in the plasmid after scaffold release was shown by the agarose gel electrophoresis experiment. The plasmid released from the scaffold and the stock plasmid had similar migration patterns. Additionally, both plasmids were linearized by the *EcoNI* restriction enzyme (Fig. 3, Lanes d and f). Supercoiling of the plasmid gives the appearance of two bands and the smearing effect on the gel (e.g. Fig. 3, Lanes b, c, e, g and h). Supercoiling causes slow band migration, therefore, it is difficult to estimate band size. Therefore, we used enzyme digestion with *EcoNI* to linearize the plasmid and allow for approximate measurement of plasmid size. The linearized plasmid size was calculated to be approximately 6.2 kb (the plasmid vector is 5.8 kb and the IGF-1 insertion was ~400b). This size is verified by the gel (Fig. 3, Lanes d and f). Although the released FG complex stock solution did migrate (Fig. 3, Lane h), it was a very light concentration compared to the stock FG complex (Fig. 3, i and g) and appears light on the image. The hydrostatic interaction with the scaffold may have allowed for the change in the migration intensity compared to the released FG complex. With the demonstrations that the IGF-1 gene is intact in the released plasmid from the scaffold

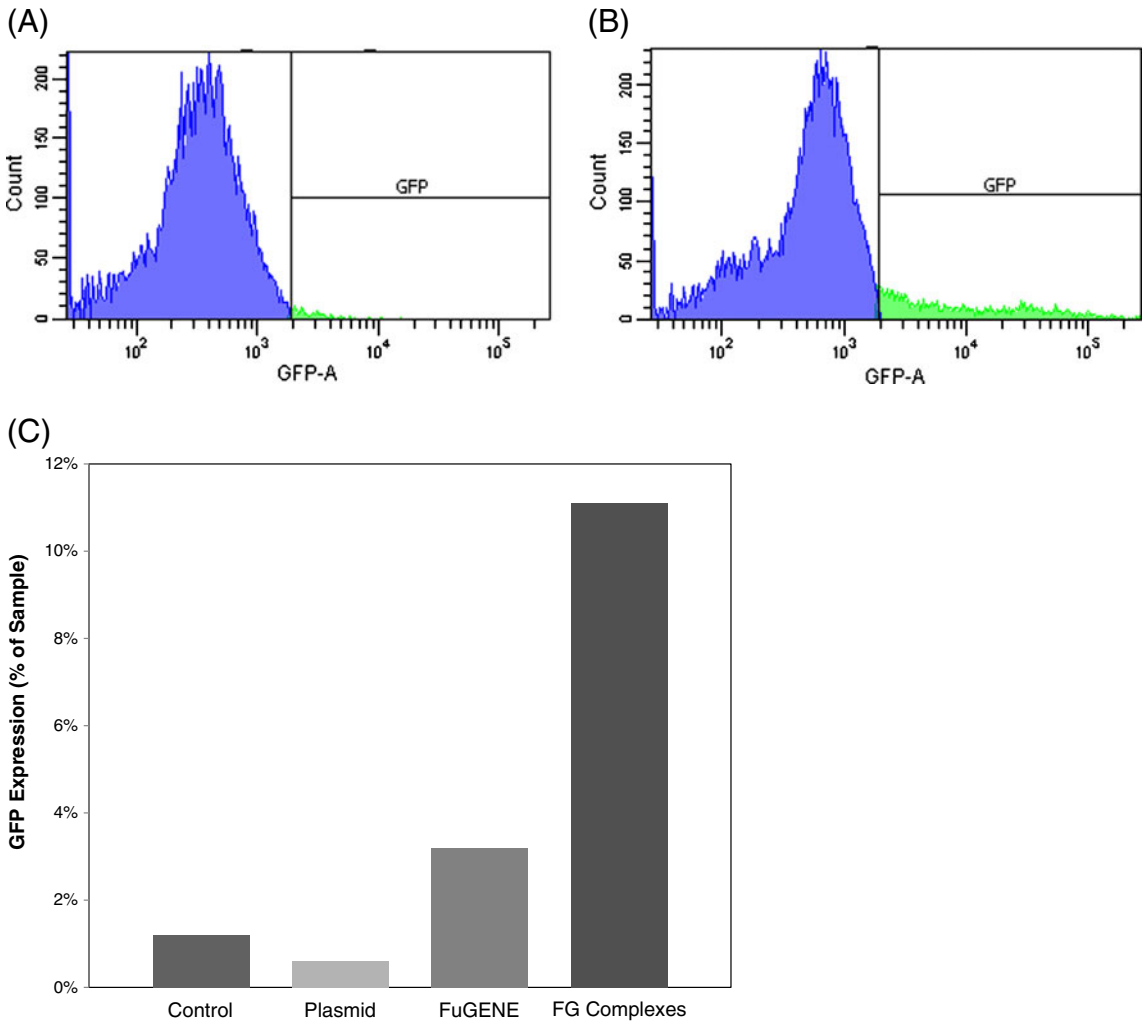

Fig. 6 (**A**) FACS histogram of control hSkMM sample expressing GFP. (**B**) FACS histogram of the transfected hSkMM sample expressing GFP. (**C**) GFP expression of control, DNA only, FuGENE only and transfected hSkMM cells.

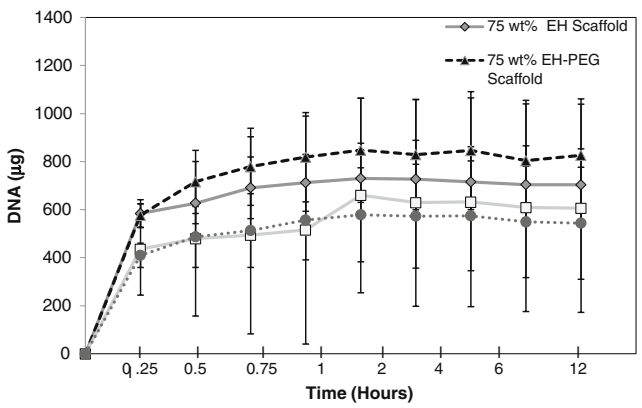

Fig. 7 Total IGF-1 GFP plasmid release from EH and EH-PEG scaffolds. Trends showed that 80 wt% EH scaffolds released more plasmid than the 75 wt% EH scaffolds. It was also observed that the porous EH-PEG scaffolds released more plasmid than their EH scaffold counterparts for up to 2 h. The 75 wt% group continued the trend for the rest of the study.

and that the stock plasmid, released plasmid and released FG complex all have similar migration characteristics, the IGF-1 gene is believed to be intact in the released plasmid and FG complex.

Once we characterized the EH and EH-PEG scaffolds, we looked to evaluate the release of a therapeutic protein, an IGF-1 GFP fusion plasmid from the scaffolds. An IGF-1 GFP fusion plasmid was constructed, and transfection studies were performed with human skeletal muscle myoblasts (hSkMMs) to test the utility and transfection ability of both the plasmid and two carriers, FG complexes and lipoplexes. After analyzing the results of the IGF-1 ELISA, we determined that all future experiments would use FG complexes due to their improved performance compared to the lipoplexes. Both GFP production and IGF-1 production in transfected hSkMMs were observed using fluorescent microscopy and an IGF-1 ELISA. Figures 5a-c show cells transfected with FG complexes

expressing GFP. Figure 5d shows the amount of IGF-1 produced by transfected hSkMMs over a 46 h incubation period. Overall, the lipoplexes and FG complexes performed similarly. There is a slight trend of increasing IGF-1 as plasmid dose increases. The 5 μg plasmid loading group was statistically higher than the control. Overall, the images of GFP production and IGF-1 ELISA results confirm that the plasmid was functional. Additionally, FACS was used to quantitatively evaluate the transfection protocol provided by the manufacturer. Approximately 10% of cells were transfected, as seen by GFP expression when treated with a ratio of 6:2 μL FuGENE reagent to μg plasmid DNA, compared to the control population with approximately 1% GFP expression (Fig. 6a and b). Additionally, three treatments, plasmid DNA only with 0.6% GFP expression, FuGENE reagent only with 3.2% GFP expression and control with 1.2% GFP expression, 0 μg plasmid DNA and 0μL FuGENE, were compared to the transfected cell population, with 11.1% GFP expression. (Fig. 6c)

Finally, to test the delivery capabilities of EH and EH-PEG scaffolds, release studies were performed. While there were no statistical differences after 24 h, some trends were evident in the data. The 75 wt% EH-PEG scaffolds released the most plasmid followed by its EH scaffold counterpart. This was expected, as more plasmid would be trapped within the network with fewer pores on the surface to leach out from. By blocking the pores with the PEG hydrogel layer, more plasmid can be retained in the network during initial loading. A similar trend was exhibited by the 80 wt% EH scaffolds and EH-PEG scaffolds during the first 2 h of release. After 2 h, the EH-PEG scaffold release leveled off, and the EH scaffolds released more complexes. Due to the high interconnectivity of these scaffolds as well as the hydrophobicity of the polymer EH, loading efficiencies were reduced to approximately 87% and 70% in the 75 wt% and 80 wt% scaffolds, respectively. When compared to the release curves of proteins from solid EH networks in previous studies, the trends remain the same, but the amount of DNA release is different (13). Therefore, it is hypothesized that loading efficiency has the highest impact on release profiles. While architectural changes do not affect the overall release trends of protein or DNA, they can indeed be an effective way to alter loading efficiencies for protein or DNA release.

These results demonstrate promise for the use of porous EH scaffolds as a gene delivery vehicle. This work shows that the release of plasmid complexes and lipoplexes can be altered based on varying scaffold architecture. By tailoring the architecture of the scaffold to hold the desired quantity of plasmid complexes or lipoplexes, one can effectively alter the complex release time and dose. Future directions involve the addition of hSkMMs to these loaded networks to determine cell behavior in the presence of EH scaffolds and EH-PEG scaffolds as well as to evaluate this scaffold *in vivo* as a therapeutic gene delivery device.

CONCLUSIONS

This work seeks to further advance the use of EH cyclic acetal biomaterials as a protein delivery device. The effect of scaffold architecture on the release of plasmid lipoplexes and complexes was evaluated. Results showed that by altering the porosity of the scaffolds, especially at the surface of the network, the release of plasmids over time could be altered. More specifically, it was shown that by modifying the surface architecture of the polymers, fast loading and lower DNA retention could be achieved with highly porous network. In addition, a therapeutic plasmid was constructed to deliver an IGF-1 GFP fusion gene to hSkMMs. When combined, these results saw a promising tunable delivery method for gene delivery to the skeletal muscle. This would allow for the EH scaffold to be used for both short-term gene therapy and a longer-term therapy as a regenerative scaffold for skeletal muscle.

ACKNOWLEDGMENTS

This work was supported by the National Science Foundation through a CAREER Award to JPF (#0448684) as well as the Maryland NanoCenter and the NispLab. The NispLab is supported in part by the NSF and as a MRSEC Shared Experimental Facility. The authors would like to thank Dr. Sameer Shah for the Lipofectamine 2000 transfection reagent and Dr. Adam Hsieh for providing ampicillin, both whom are at the University of Maryland. We would also like to thank Chen-Yu Tsao, Chi-Wei Hung and Hsuan-Chen Wu from the lab of Dr. William Bentley at University of Maryland for their contributions.

REFERENCES

1. Delieand F, Blanco-Prieto MJ. Polymeric particulates to improve oral bioavailability of peptide drugs. Molecules. 2005;10:65–80.
2. Hoffman AS. "Intelligent" polymers in medicine and biotechnology. Artif Organs. 1995;19:458–67.
3. Galaevand IY, Mattiasson B. 'Smart' polymers and what they could do in biotechnology and medicine. Trends Biotechnol. 1999;17:335–40.
4. Breen A, O'Brien T, Pandit A. Fibrin as a delivery system for therapeutic drugs and biomolecules. Tissue Eng Part B Rev. 2009;15(2):201–14.
5. Falco EE, Patel M, Fisher JP. Recent developments in cyclic acetal biomaterials for tissue engineering applications. Pharm Res. 2008;25:2348–56.
6. Raghunath J, Rollo J, Sales KM, Butler PE, Seifalian AM. Biomaterials and scaffold design: key to tissue-engineering cartilage. Biotechnol Appl Biochem. 2007;46:73–84.

7. Lendlein A, Kratz K, Kelch S. Smart implant materials. Med Device Technol. 2005;16:12–4.
8. Sachlosand E, Czernuszka JT. Making tissue engineering scaffolds work. Review: the application of solid freeform fabrication technology to the production of tissue engineering scaffolds. Eur Cell Mater. 2003;5:29–39. discussion 39-40.
9. Moreau JL, Kesselman D, Fisher JP. Synthesis and properties of cyclic acetal biomaterials. J Biomed Mater Res A. 2006.
10. Kaihara S, Matsumura S, Fisher JP. Synthesis and properties of Poly[poly(ethylene glycol)-co-cyclic acetal] based hydrogels. Macromolecules. 2007;40:7625–32.
11. Nair L, Laurencin C. Biodegradable polymers as biomaterials. Prog Polym Sci. 2007;32:762–98.
12. Kaihara S, Matsumura S, Fisher JP. Synthesis and characterization of cyclic acetal based degradable hydrogels. Eur J Pharm Biopharm. 2008;68:67–73.
13. Falco EE, Roth JS, Fisher JP. EH Networks as a scaffold for skeletal muscle regeneration in abdominal wall hernia repair. J Surg Res. 2008;149:76–83.
14. Betz MW, Modi PC, Caccamese JF, Coletti DP, Sauk JJ, Fisher JP. Cyclic acetal hydrogel system for bone marrow stromal cell encapsulation and osteodifferentiation. J Biomed Mater Res A. 2008;86:662–70.
15. Braun S. Muscular gene transfer using nonviral vectors. Curr Gene Ther. 2008;8:391–405.
16. Lee Y, Park EJ, Yu SS, Kim DK, Kim S. Improved expression of vascular endothelial growth factor by naked DNA in mouse skeletal muscles: implication for gene therapy of ischemic diseases. Biochem Biophys Res Commun. 2000;272:230–5.
17. Musarò A, Giacinti C, Borsellino G, Dobrowolny G, Pelosi L, Cairns L, *et al.* Stem cell-mediated muscle regeneration is enhanced by local isoform of insulin-like growth factor 1. Proc Natl Acad Sci USA. 2004;101:1206.
18. DeVol DL, Rotwein P, Sadow JL, Novakofski J, Bechtel PJ. Activation of insulin-like growth factor gene expression during work-induced skeletal muscle growth. Am J Physiol. 1990;259:E89–95.
19. Beguinot F, Kahn CR, Moses AC, Smith RJ. Distinct biologically active receptors for insulin, insulin-like growth factor I, and insulin-like growth factor II in cultured skeletal muscle cells. J Biol Chem. 1985;260:15892–8.
20. Barton-Davis ER, Shoturma DI, Sweeney HL. Contribution of satellite cells to IGF-I induced hypertrophy of skeletal muscle. Acta Physiol Scand. 1999;167:301–5.
21. Mourkiotiand F, Rosenthal N. IGF-1, inflammation and stem cells: interactions during muscle regeneration. Trends Immunol. 2005;26:535–42.
22. Hashimoto N, Murase T, Kondo S, Okuda A, Inagawa-Ogashiwa M. Muscle reconstitution by muscle satellite cell descendants with stem cell-like properties. Development. 2004;131:5481–90.
23. Adamsand GR, McCue SA. Localized infusion of IGF-I results in skeletal muscle hypertrophy in rats. J Appl Physiol. 1998;84:1716–22.
24. Barton-Davis ER, Shoturma DI, Musaro A, Rosenthal N, Sweeney HL. Viral mediated expression of insulin-like growth factor I blocks the aging-related loss of skeletal muscle function. Proc Natl Acad Sci USA. 1998;95:15603–7.
25. Thomas C, Ehrhardt A, Kay M. Progress and problems with the use of viral vectors for gene therapy. Nat Rev Genet. 2003;4:346–58.
26. Vermaand I, Weitzman M. Gene therapy: twenty-first century medicine. Biochemistry. 2005;74:711–38.
27. Grunwaldand S, Speer A. Efficient transfection of primary human skeletal myoblasts using FuGENE® HD transfection reagent. Gene Expr. 2007;3:26.
28. Arnold A, Laporte V, Dumont S, Appert-Collin A, Erbacher P, Coupin G, *et al.* Comparing reagents for efficient transfection of human primary myoblasts: FuGENE 6, Effectene and ExGen 500. Fundam Clin Pharmacol. 2006;20:81–9.
29. Ye L, Haider H, Esa W, Law P, Zhang W, Su L, *et al.* Nonviral vector-based gene transfection of primary human skeletal myoblasts. Exp Biol Med (Maywood, NJ). 2007;232:1477.